



Semnan University



## Research Article

# Thermal and Rheological Analysis of Elliptical Ducts and Non-Newtonian Nanofluids in Heat Exchanger Applications

Dounya Behnous <sup>a</sup> , Haroun Ragueb <sup>b</sup> , Belkacem Manser <sup>b</sup>Antar Tahiri <sup>c</sup>, Kacem Mansouri <sup>a</sup><sup>a</sup> Laboratory of Physical Engineering of Hydrocarbons, Faculty of Hydrocarbons and Chemistry, University M'hamed Bougara of Boumerdes, 35000, Boumerdes, Algeria<sup>b</sup> Laboratory of Energy and Mechanical Engineering (LEMI), Faculty of Technology, University M'Hamed Bougara of Boumerdes, 35000, Boumerdes, Algeria<sup>c</sup> Laboratory of Mechanical and Materials Development, LDMM, University of Djelfa, Djelfa 17000, Algeria

## ARTICLE INFO

**Article history:**

Received: 2025-04-18

Revised: 2025-07-19

Accepted: 2025-08-16

**Keywords:**

Elliptical ducts;

Non-Newtonian nanofluids;

Heat exchanger performance;

Thermal efficiency;

Double pipe heat exchanger.

## ABSTRACT

This study numerically investigates the thermal and rheological performance of a double-pipe heat exchanger (DPHE) with an inner elliptical duct (with an aspect ratio of 0.25) using non-Newtonian nanofluids comprising multi-walled carbon nanotubes (MWCNTs) dispersed in water, stabilized with 0.2 wt.% cationic chitosan. Employing the finite volume method, we demonstrate that elliptical ducts significantly enhance heat transfer compared to circular tubes, increasing the number of transfer units (NTU) by up to 25% and effectiveness by 17%. The incorporation of MWCNTs further improves heat transfer by enhancing thermal conductivity, achieving up to 30% increase in NTU and 20% in effectiveness. Despite higher pressure losses in elliptical ducts, the shear-thinning behavior of the nanofluids mitigates these losses at higher flow rates, reducing pumping power requirements. These findings highlight the potential of combining elliptical ducts and non-Newtonian nanofluids to optimize DPHE efficiency, offering significant implications for energy-efficient heat exchanger designs in industrial applications.

© 2025 The Author(s). Journal of Heat and Mass Transfer Research published by Semnan University Press.

This is an open access article under the CC-BY-NC 4.0 license. (<https://creativecommons.org/licenses/by-nc/4.0/>)

## 1. Introduction

Heat exchangers are ubiquitous devices, seamlessly integrated into our everyday appliances such as refrigerators, air conditioners, automobiles, and even coffee makers. They are also essential components in various industrial settings, including power plants, nuclear facilities, oil refineries, and food processing factories. In response to the growing demand for energy and mounting environmental concerns, researchers globally are actively working to improve heat transfer within heat exchangers

and promote energy conservation [1]. To achieve these goals, two fundamental techniques are employed.

The first is known as the active technique, which involves the utilization of external heat sources, albeit at the cost of additional energy consumption. The second technique, referred to as the passive technique, does not rely on external energy sources. Instead, it improves heat exchange by expanding the exchange surface, inserting turbulators, or augmenting the thermal properties of the working fluids.

**\* Corresponding author.***E-mail address:* [d.behnous@univ-boumerdes.dz](mailto:d.behnous@univ-boumerdes.dz)**Cite this article as:**Behnous, D., Ragueb, H., Manser, B., Tahiri, A. and Mansouri, K. 2026. Thermal and Rheological Analysis of Elliptical Ducts and non-Newtonian Nanofluids in Heat Exchanger Applications. *Journal of Heat and Mass Transfer Research*, 13(1), pp. 73-88.<https://doi.org/10.22075/JHMTR.2025.37428.1722>

The double pipe heat exchanger (DPHE) is widely popular due to its cost-effectiveness, simplicity, operational ease, and ability to handle high pressure and temperature. It is used across various industries, including food processing, chemical manufacturing, pharmaceuticals, and more [2, 3]. Scholars have proposed numerous techniques to enhance the efficiency of this category of heat exchanger, with a key focus on the use of passive techniques to improve heat transfer. Many methods have been recommended to extend the heat transfer area. Huu-Quan et al. [4] investigated turbulent forced convective heat transfer in double-pipe heat exchangers featuring flat inner pipes. They noted that flat tubes inherently possess a larger surface area compared to round tubes, even when they share the same cross-sectional area. They discovered that for Reynolds numbers below 7000, employing flat inner pipes with a low aspect ratio was beneficial, resulting in increases of approximately 2.9% in the overall convective heat transfer coefficient, 2.7% in thermal effectiveness, and 16.8% in the performance index. Conversely, for  $Re > 7000$ , circular inner pipes outperformed flat ones, indicating that the choice of inner pipe geometry should be based on Reynolds number considerations for heat exchanger design. Zhang et al. [5] utilized numerical simulations with the  $k-\varepsilon$  model to examine thermal response and fluid flow in a cross-combined dimple tube, proposing a novel enhancement model based on composite-shaped surfaces. The main function of these dimples is to augment the heat transfer area and induce turbulence in the flow. Their findings showed that compared to a single ellipsoidal dimple tube, heat transfer increased by 18.8–48.3%, with an average of 24.8%. Corcoles et al. [6] explored the influence of geometric variations through 3D numerical simulations, analyzing how different designs of eight spirally corrugated inner tubes impact performance in a double-pipe heat exchanger under turbulent flow ( $Re = 25,000$ ). They explored various combinations of pitch and height for the corrugated tubes, with particular emphasis on the enhanced heat exchange capabilities provided by the larger surface area of the corrugated tubes. Luo et al. [7] delved into the performance of a double-pipe heat exchanger design featuring two oval pipes with varying twist pitches. Their numerical analysis in the laminar flow regime revealed that as the twist pitch ratio between the outer and inner pipes grew, heat transfer initially surged before tapering off. Notably, the increase in flow resistance was much less pronounced than the heat transfer boost. The most remarkable improvement occurred at a twist pitch ratio of 1.5, where the Nusselt number rose by 97.0%,

while the friction factor only climbed by 43.7%, outperforming a standard straight annular pipe.

On the other hand, many scholars are actively exploring the utilization of turbulators (vortex generators) as an innovative and highly effective approach to enhance turbulence, thereby leading to improved heat transfer characteristics [8]. Karaouei and Ajarostaghi [9] introduced a new design for a double-coil heat exchanger, incorporating an innovative curved swirl generator in the inner channel. Their investigation revealed that enlarging the inner radius of the turbulator by 26.7% could amplify effectiveness by a remarkable 80%. Meanwhile, increasing the radius of the turbulator's holes by 133.34% resulted in a more modest yet still impressive 50% boost in effectiveness, both at controlled mass flow rates. Noorbakhsh et al. [10] explored numerically the impact of varying twisted tape geometries in both tubes of a double-pipe heat exchanger to enhance heat transfer. They discovered that adding more twisted tapes, ranging from one to four, boosted the Nusselt number by 3.1%. However, this gain in heat transfer came at a cost: pressure drop surged by 64%, and the coefficient of performance dropped by 63.9%. Nakhchi et al. [11] investigated the enhancement of heat transfer and entropy generation in double-pipe heat exchangers by employing turbulent nanofluids combined with innovative perforated cylindrical turbulators. They found that these perforated turbulators achieved a considerably higher thermal performance factor. In a second study [8], the authors examined the thermal performance of double-pipe heat exchangers enhanced with innovative double perforated inclined elliptic turbulators. Their results revealed a significant boost in heat transfer, with the turbulators increasing the average Nusselt number by an impressive 217.4% compared to tubes without vortex generators.

Following Eastman et al.'s pioneering work [12], which demonstrated that adding nanoparticles to a fluid creates a nanofluid with significantly improved thermal properties, especially a marked increase in thermal conductivity, numerous researchers have since focused on integrating nanofluids into heat exchanger designs to make use of these enhanced performance characteristics [13-16]. Noorbakhsh et al. [17] used numerical simulations to delve into heat transfer enhancement in a DPHE outfitted with twisted tapes acting as swirl generators on both the hot and cold sides. They tested three nanofluids (water-based mixtures with  $Al_2O_3$ ,  $CuO$ , and  $SiO_2$  nanoparticles), flowing through the hot stream. Their findings revealed that  $CuO$ /water nanofluid outperformed the others, showing a remarkable

7% improvement in thermal performance compared to pure water at  $Re = 5492$ . Meanwhile, SiO<sub>2</sub>/water nanofluid delivered the least enhancement (2.5%) at  $Re = 3343$ . Additionally, they noted that the choice of nanoparticle concentration affected thermal performance differently at lower and higher Reynolds numbers. Bahmani et al. [18] explored forced convection in a DPHE using nanofluids with both constant and variable thermophysical properties. In their study, distilled water flowed through the annulus, while Al<sub>2</sub>O<sub>3</sub>/water nanofluid circulated in the inner tube. Their findings revealed that increasing the nanoparticle volume fraction and Reynolds number significantly enhanced the heat transfer rate. However, they also found that thermal efficiency was superior when thermophysical properties were treated as constant, while the average Nusselt number was higher when variable properties were considered.

Recently, researchers have been drawn to the exploration of multi-walled carbon nanotubes (MWCNTs) due to their exceptional thermal conductivity, sparking significant interest in their study and application in various fields [19-23]. In their experimental study, Moradi et al. [24] explored the heat transfer behavior of MWCNTs/water nanofluids within a countercurrent DPHE, enhanced by porous media. They uncovered that integrating plate porous media led to a substantial increase in the heat transfer coefficient, with the greatest improvement of 35% occurring at the lowest nanofluid mass fraction of 0.04%. Karaoui et al. [25] carried out a numerical study to assess the thermal performance of a helical DPHE, enhanced by a novel curved turbulator and two types of hybrid nanofluids: silver-graphene/water and MWCNT-Fe<sub>3</sub>O<sub>4</sub>/water. Their findings revealed that the heat exchanger's thermal efficiency was at its lowest with a volume concentration of  $\phi = 0.1\%$ , while it reached its peak at  $\phi = 0.7\%$ . Fathian et al. [26] performed an experimental study to examine the effect of adding single-walled and multi-walled carbon nanotubes to distilled water in helical annuli, utilizing a DPHE with different coil geometries. They discovered that the nanofluid flow produced significantly higher Nusselt numbers compared to the base fluid flow. Additionally, they developed a correlation to predict Nusselt numbers, which showed a good agreement with the experimental data, offering a reliable tool for heat transfer prediction in similar systems.

In addition, the introduction of nanoparticles into a base fluid has a profound impact on its viscosity and rheological behavior [27-30]. Depending on factors such as the base fluid type and the shape, size, and characteristics of the

nanoparticles, some nanofluids exhibit a typical Newtonian flow behavior [31-34], while others demonstrate non-Newtonian characteristics [35, 36]. Existing literature shows that, in most cases, non-Newtonian nanofluids exhibit shear-thinning behavior as the nanoparticle concentration increases [37-40]. However, in certain instances, an opposite trend is observed, where shear thickening behavior becomes more pronounced as the nanoparticle concentration rises [41-46], adding complexity to the fluid dynamics.

In this context, the use of elliptical ducts and nanofluids can be classified as passive techniques, as they do not require external energy sources. For a given cross-sectional area, an ellipse has a larger perimeter than a circle, which enhances the flow dynamics and heat transfer. Early theoretical studies on forced convection in elliptical ducts demonstrated that flattening the duct, while maintaining a constant cross-sectional area, significantly improves the heat transfer coefficient [47-50]. This effect highlights the potential of elliptical ducts as an effective means of optimizing heat transfer without the need for additional energy input. The experiment conducted by Abdel-Wahed et al. [51] validated the Nusselt number enhancement predicted by the theoretical work of Javeri [52]. On the other hand, numerous experiments and numerical studies [53-58] have highlighted the remarkable thermal performance of elliptic tube bundles in crossflow, showing that their use in heat exchangers can lead to substantial improvements. For instance, Matos et al. [53, 54] found that elliptic tubes could boost heat transfer by up to 20%, while Li et al. [55] observed a significant 30-40% reduction in pressure drop compared to conventional circular ducts. With such impressive efficiency gains, Ibrahim and Gomaa [56] concluded that heat exchangers featuring elliptic tube bundles play a key role in advancing energy conservation efforts, offering a promising path toward more sustainable designs.

Previous studies have consistently shown that elliptical ducts with an aspect ratio of 0.25 offer superior thermal performance [21, 47, 49]. Building on this foundation, our study investigates the potential of combining elliptical ducts with an aspect ratio of 0.25 and non-Newtonian nanofluids to further enhance heat exchanger efficiency. To this end, we develop a numerical model of a double-pipe co-current heat exchanger using the finite volume method. We then conduct a comparative analysis of the thermal performance between elliptical ducts and traditional circular tubes. In addition, we explore how nanoparticle concentration and rheological behavior influence thermal performance, focusing on non-Newtonian

nanofluids consisting of MWCNTs dispersed in water and stabilized with 0.2 wt.% cationic chitosan. This approach is novel as it synergistically combines the enhanced heat transfer surface of elliptical ducts with the superior thermal conductivity and shear-thinning properties of non-Newtonian nanofluids, offering a passive technique to significantly improve DPHE performance without external energy input. The next section outlines the mathematical model and numerical approach used in our study, followed by a detailed description of the methodology for assessing the heat exchanger's thermal performance. Section 4 delves into the thermal and rheological behavior of the non-Newtonian nanofluids, and Section 5 presents an in-depth discussion of the results. The paper concludes with a summary of the key findings.

## 2. Model Description and Numerical Method

### 2.1. Description of the Double-Pipe Heat Exchanger

To investigate the performances of elliptical ducts in heat exchanger applications, we consider two DPHEs: one is equipped with an inner elliptical tube with an aspect ratio of 0.25, and the second is fitted with a circular pipe. A schematic geometry of the considered DPHE is shown in Fig. 1.

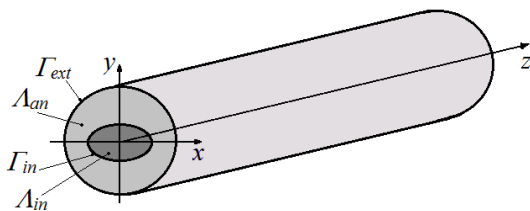


**Fig. 1.** Schematic geometry of the double-pipe heat exchanger with elliptical tube

For fair comparisons, the external tube is always circular with a constant diameter  $D_{ext}$ ; however, the inner tube can be either circular or elliptical with the same cross-section area  $A_{in}$ . The interface  $\Gamma_{in}$ , between the annular space  $A_{an}$ , and the inner space  $A_{in}$ , has no significant thermal resistance (the interface thickness is zero), whereas the external wall  $\Gamma_{ext}$ , is adiabatic. Both the hot and the cold fluid enter from the same side at  $z = 0$  (co-current configuration), with constant temperature and uniform velocity. This geometry is relevant to engineering processes, such as compact heat exchanger designs in chemical processing and HVAC systems, where elliptical ducts are advantageous due to their

ability to fit in constrained spaces while maximizing heat transfer surface area. The geometrical parameters of the two heat exchangers are listed in Table 1.

**Table 1.** Geometric parameters of the considered double-pipe heat exchangers

Parameters	DPHE with circular tube	DPHE with elliptical tube
Dext (mm)	30	30
a (mm)	10	20
b (mm)	10	05
L (mm)	2000	2000
$A_{in}$ (mm <sup>2</sup> )	78.54	78.54
$A_{an}$ (mm <sup>2</sup> )	628.32	628.32
S (m <sup>2</sup> )	0.06283	0.08590
Dh,in (mm)	10	7.31
Dh,an (mm)	20	18.32

### 2.2. Mathematical Modeling

To solve the coupled system of fluid flow and heat transfer, the following assumptions are made to simplify the numerical resolution:

- The thermo-physical properties are thermo-independent and constant;
- The flow is incompressible, single-phase and laminar;
- Effects of gravity and other body forces are neglected, as well as viscous dissipation and axial conduction;
- Both the heat transfer and the fluid flow are in a steady-state.

Based on the above assumptions and the heat exchanger geometry, the governing equations are derived from fundamental principles of fluid dynamics and heat transfer [59], and expressed as follows:

- At the inner tube, the continuity, the momentum and the energy equations are given as, respectively [59]:

$$\nabla \cdot (\rho_{in} \vec{V}_{in}) = 0 \quad (1)$$

$$\rho_{in} (\vec{V}_{in} \cdot \nabla \vec{V}_{in}) = -\nabla p_{in} + \nabla \cdot \left( \frac{\mu_{in}}{2} (\nabla \vec{V}_{in} + \nabla^T \vec{V}_{in}) \right) \quad (2)$$

$$\rho_{in} C_{p_{in}} (\vec{V}_{in} \cdot \nabla T_{in}) = \kappa_{in} \nabla^2 T_{in} \quad (3)$$

subject to the following inlet and boundary conditions (inlet velocity, no-slip boundary condition, outlet pressure, and inlet boundary condition, respectively) [59]:

$$\|\vec{V}_{in}\| = V_{0,in}, (x, y) \in \Lambda_{in} \ \& \ z = 0 \quad (4)$$

$$\vec{V}_{in} = \vec{0}, (x, y, z) \in \Gamma_{in} \quad (5)$$

$$p_{in} = p_o, (x, y) \in \Lambda_{in} \ \& \ z = L \quad (6)$$

$$T = T_{0,in}, (x, y) \in \Lambda_{in} \ \& \ z = 0 \quad (7)$$

- At the annular space, the continuity, momentum and energy equations are defined as [59]:

$$\nabla \cdot (\rho_{an} \vec{V}_{an}) = 0 \quad (8)$$

$$\rho_{an} (\vec{V}_{an} \cdot \nabla \vec{V}_{an}) = -\nabla p_{an} + \nabla \cdot \left( \frac{\mu_{an}}{2} (\nabla \vec{V}_{an} + \nabla^T \vec{V}_{an}) \right) \quad (9)$$

$$\rho_{an} C p_{an} (\vec{V}_{an} \cdot \nabla T_{an}) = \kappa_{an} \nabla^2 T_{an} \quad (10)$$

with the following corresponding inlet and boundary conditions (inlet velocity, no-slip boundary condition, pressure outlet condition, inlet temperature and adiabatic external wall, respectively) [59]:

$$\|\vec{V}_{an}\| = V_{0,an}, (x, y) \in \Lambda_{an} \ \& \ z = 0 \quad (11)$$

$$\vec{V}_{an} = \vec{0}, (x, y, z) \in \Gamma_{in} \ \vee \ \Gamma_{ext} \quad (12)$$

$$p_{an} = p_o, (x, y) \in \Lambda_{an} \ \& \ z = L \quad (13)$$

$$T = T_{0,an}, (x, y) \in \Lambda_{an} \ \& \ z = 0 \quad (14)$$

$$-\kappa_{an} \frac{\partial T_{an}}{\partial \xi} = 0, (x, y) \in \Gamma_{ext} \ \& \ \xi \perp \Gamma_{ext} \quad (15)$$

- At the interface that separates the inner space and the annular space,  $\Gamma_{in}$  (See Fig. 1), a coupling condition is imposed to ensure the heat transfer between the inner fluid and the outer one as follows [59]:

$$\begin{cases} -\kappa_{in} \frac{\partial T_{in}}{\partial \zeta} = \kappa_{an} \frac{\partial T_{an}}{\partial \zeta}, & (x, y, z) \in \Gamma_{in} \\ & \& \ \zeta \perp \Gamma_{in} \\ T_{w,in} = T_{w,an} = T_w, & (x, y, z) \in \Gamma_{in} \end{cases} \quad (16)$$

In case of a non-Newtonian fluid, the viscosity is described by the power-law model as follows [60]:

$$\mu = K (\dot{\gamma})^{\eta-1} \quad (17)$$

where  $K$  is the consistency coefficient, and  $\eta$  is the flow behavior index. The power-law model was chosen for its simplicity and accuracy in

capturing the shear-thinning behavior of MWCNT-water nanofluids, as validated by experimental data [36, 40].

### 2.3. Numerical Resolution

The above set of nonlinear PDEs and boundary conditions is solved using the Finite Volume Method (FVM)[59, 61]. FVM was selected due to its robustness in handling complex geometries and coupled fluid-thermal problems, offering advantages over analytical methods, which are less practical for non-linear, non-Newtonian flows in elliptical ducts [61]. The discretization of the convective and diffusive terms has been done using the second order upwind method, whereas the pressure and the velocity were decoupled using the Semi Implicit Method for Pressure Linked Equations, SIMPLE [59]. For all cases treated in this study, the solution is considered convergent if all residuals (momentum, continuity, and energy) are less than  $10^{-6}$ , ensuring the robustness and accuracy of the numerical approach.

### 3. Heat Transfer Characteristics

The quantity of heat exchanged by the hot and the cold fluids during their passage through the DPHE is defined as flow [62]:

$$Q_h = \dot{m}_h C p_h (\bar{T}_{h,i} - \bar{T}_{h,o}) = C_h (\bar{T}_{h,i} - \bar{T}_{h,o}) \quad (18)$$

$$Q_c = \dot{m}_c C p_c (\bar{T}_{c,i} - \bar{T}_{c,o}) = C_c (\bar{T}_{c,i} - \bar{T}_{c,o}) \quad (19)$$

Since our heat exchanger has no thermal resistance at the interface, the amount of heat yielded by the hot fluid is equal to the quantity absorbed by the cold fluid, thus the effectiveness of the heat exchanger can be written as flow [62]:

$$\varepsilon = \frac{C_h (\bar{T}_{h,i} - \bar{T}_{h,o})}{C_{min} (\bar{T}_{h,i} - \bar{T}_{c,i})} = \frac{C_c (\bar{T}_{c,o} - \bar{T}_{c,i})}{C_{min} (\bar{T}_{h,i} - \bar{T}_{c,i})} \quad (20)$$

where the mean inlet and outlet temperatures can be computed as follows [61]:

$$\bar{T} = \frac{1}{\Lambda \times V_{av} \ \Lambda} \int \|\vec{V}(x, y)\| \times T(x, y) ds \quad (21)$$

The average heat transfer coefficients from both sides of the interface, the cold side and the hot side are given as, respectively:

$$\bar{h}_c = \frac{Q_c}{S(T_{w,av} - T_{b,c})} \quad (22)$$

$$\bar{h}_h = \frac{Q_h}{S(T_{b,h} - T_{w,av})} \quad (23)$$

here,  $T_{w,av}$  is the interface average temperature, and  $T_b$  is the fluid bulk temperature.

The two temperatures are computed as follows, respectively [62]:

$$T_{w,av} = \frac{1}{S} \int_S T_w ds \quad (24)$$

$$T_b = \frac{1}{\Lambda \times L \times V_{av}} \int_{\Lambda \times L} \|\vec{V}(x, y, z)\| \times T(x, y, z) dv \quad (25)$$

The average Nusselt number for any side is given by [63-65]:

$$Nu = \frac{\bar{h} D_h}{\kappa} \quad (26)$$

The overall heat transfer coefficient as well as the number of transfer units, *NTU*, are computed as follows, respectively [62]:

$$U = \frac{\bar{h}_h \times \bar{h}_c}{\bar{h}_h + \bar{h}_c} \quad (27)$$

$$NTU = \frac{US}{C_{min}} \quad (28)$$

#### 4. Thermo-Physical Properties of Nanofluids

The addition of MWCNTs to a fluid has mainly two effects: one, augmentation of the thermal conductivity, and two, the shear-thinning behavior. In this study, a non-Newtonian nanofluid consisting of MWCNTs dispersed in water and stabilized by adding 0.2 wt% of cationic chitosan as a stabilizer is considered [40]. This nanofluid strongly exhibits shear-thinning behavior as the percentage of nanotubes increases [39-42].

The thermal and rheological data of MWCNT/water nanofluid needed in the following simulations have been extracted from [40], and presented in Table 2. The power-law model used here offers advantages such as simplicity and accuracy in modeling shear-thinning behavior, but it has limitations, including its inability to capture complex rheological behaviors at very low or high shear rates [66].

**Table 2.** Power law indices and thermal conductivity measurements for MWCNT-water with respect to mass concentration [40]

$\varphi$ (wt. %)	$\phi$ (vol %)	K (Pa.sn)	$\eta$ (-)	$\kappa$ (W/mK)
0.00	0.00	0.0113	1.0000	0.589
1.00	0.48	0.0167	0.8831	0.606
2.00	0.95	0.2725	0.5078	0.621
3.00	1.43	0.7711	0.3023	0.656

#### 5. Simulation Results and Discussions

Mesh size has a significant influence on results quality. To guarantee their accuracy, several grid sizes have been tested to select an appropriate sizing so that for each simulation, the outputs are independent of grid size. In this test, we consider only the base fluid flowing in both annular and inner space with the same inlet velocity,  $V_{0,in,an} = 0.01$  m/s. The fluid entering the inner duct has a temperature  $T_{0,in} = T_{c,i} = 300$  K, whereas the one entering the annular space has an inlet temperature  $T_{0,an} = T_{h,i} = 350$  K. The heat exchanger mesh consists of a sweep with a fixed step along the z-axis of the quadrilateral mesh in the cross-section presented in Fig. 2.

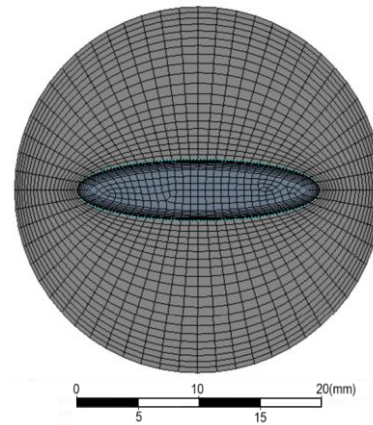


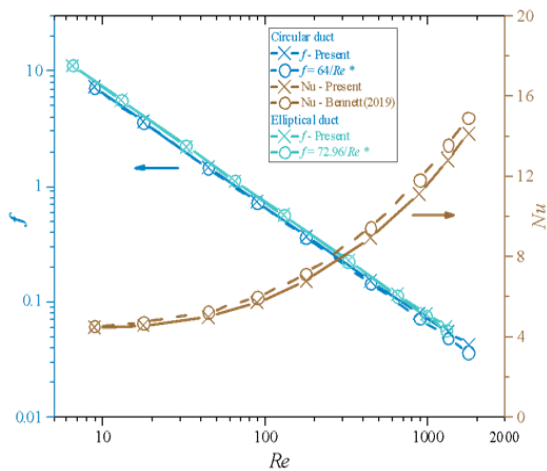
**Fig. 2.** Mesh in the cross-section of the heat exchanger

Four mesh settings, namely, M1, M2, M3, and M4 have been considered, and the simulation results are presented in Table 3. To ensure accuracy and reliability of the present numerical model, for each mesh setting, we have computed several parameters, which are listed in Table 3, for comparisons and analysis.

Theoretically, since our heat exchanger is ideal, with no heat losses at walls, the amount of heat absorbed by the cold fluid must be the same as the one yielded by the hot fluid if the simulation is working correctly ( $Q_c = Q_h$ ). In Table 3 we observe that the deviation between  $Q_c$  and  $Q_h$  narrows as the mesh size increases, and in all cases the deviation is less than 0.4%. This means that our numerical model translates with high fidelity the physical behavior of an ideal heat exchanger. In addition, we have computed the deviation between different parameters obtained with M3 and M4. As shown in the last column, the gaps between the computed results are less than 0.6%. Since M3 requires less CPU time and memory usage than M4 (30% in time consumption, and 15% in the number of nodes and elements), the mesh M3 is the one used in the remaining part of this study for both cases of elliptical and circular inner duct.

**Table 3.** Mesh size influence on thermal and hydraulic parameters

	M1	M2	M3	M4	Dev (M3 vs. M4)
Nodes	1056055	1648647	1924923	2215213	--
Elements	995000	1569000	1833000	2111000	--
$\bar{T}_{h,o}$ (K)	344.896	344.892	344.890	344.888	0.00%
$\bar{T}_{c,o}$ (K)	340.987	340.950	340.943	340.938	0.00%
$Q_h$ (W)	133.633	133.744	133.799	133.834	0.03%
$Q_c$ (W)	134.135	134.013	133.990	133.976	0.01%
Dev ( $Q_h$ vs. $Q_c$ )	0.38%	0.20%	0.14%	0.11%	--
$\bar{h}_h$ (W/m <sup>2</sup> K)	-171.070	-172.325	-173.198	-173.331	0.08%
$\bar{h}_c$ (W/m <sup>2</sup> K)	271.501	272.571	273.796	275.354	0.57%
$\Delta p_{an}$ (Pa)	27.740	27.800	27.790	27.770	0.11%
$\Delta p_{in}$ (Pa)	149.410	150.300	151.500	151.790	0.19%
NTU	2.755	2.771	2.785	2.792	0.27%
CPU time (s)	1884.4	1345.2	2814.6	3866.1	--

**Fig. 3.** Model Validation: comparative analysis of Darcy friction and Nusselt number for circular and elliptical duct

To validate the model predictions, Fig. 3 presents a comparison between our obtained data and the Darcy friction factor correlation for circular and elliptical ducts in laminar flow, as well as the Nusselt number for the circular duct. As can be seen, the use of mesh M3 produces excellent predictions of the Darcy friction factor for various Reynolds numbers in both elliptical and circular ducts. Additionally, the obtained

Nusselt number is highly satisfactory. Notably, at higher Reynolds numbers, our model's computed Nusselt number is lower than Bennett's correlation [67]. This is expected, as Bennett's correlation assumes constant heat flux conditions, whereas our configuration involves heat exchange with an external fluid, leading to a lower Nusselt number [67].

It is important to note that Bennett's correlation predicts the Nusselt number for laminar flow in a circular duct under constant heat flux conditions [67]. In our configuration, the duct exchanges heat with the external fluid, and constant heat flux does not apply. Hence, the Nusselt number should be lower compared to the case of constant heat flux, as predicted by our model. The figure serves as evidence of the accuracy and reliability of our numerical model.

To investigate the performances of using elliptical duct as well as nanofluids in DPHE, we consider the following assumptions:

- In the annular space, only the base fluid flows with constant inlet velocity and temperature,  $V_{0,an} = 0.01$  m/s and  $T_{0,an} = T_{h,i} = 350$  K, in all cases.

- The inner pipe can be either elliptical with  $\beta/\alpha = 0.25$  or circular,  $\beta/\alpha = 1$ , where the geometrical characteristics are as shown in Table 1.
- Only the base fluid flows in the circular inner pipe, whereas the non-Newtonian nanofluids flow within the elliptical duct so as to investigate the combined performances.
- The inlet velocity in the inner duct varies from 0.01 m/s to 2 m/s within the boundary of laminar regime, and with fixed inlet temperature,  $T_{0,in} = T_{c,i} = 300$  K.
- The MWCNTs loading in the base fluid varies from 0 to 3% wt.

Using the M3 mesh setting for both elliptical and circular inner duct, and varying inlet velocity and the nanoparticles loading, the computed outlet temperature and the amount of heat exchanged are depicted in Fig. 4.

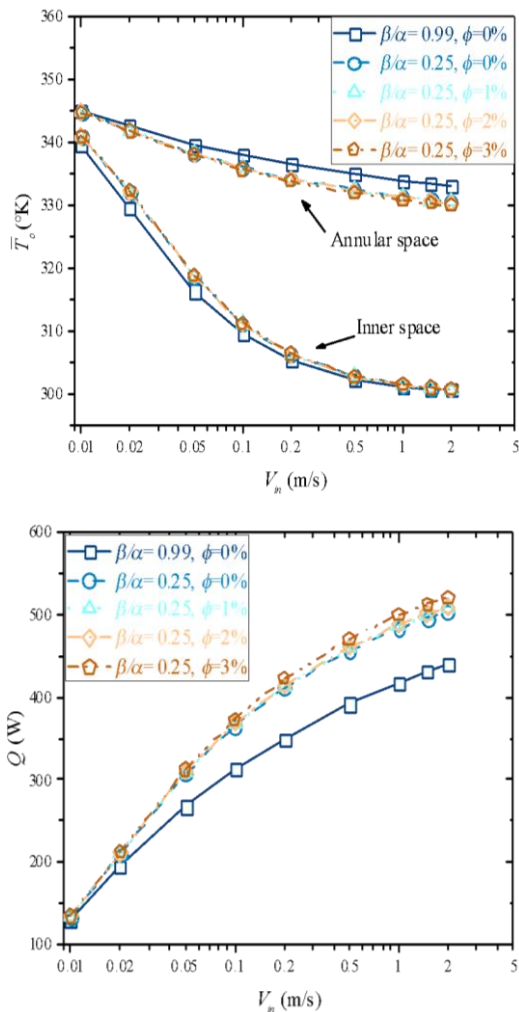


Fig. 4. Evolution of the average outlet temperature (top) and the heat transferred (bottom) in the heat exchanger according to the inlet velocity

As shown in the left curves, the use of elliptical duct decreases the outlet temperature of the hot

fluid flowing in the annular space compared to the circular duct, and it decreases more as the inlet velocity increase. This means that the use of elliptical duct allows evacuating more heat compared to the circular duct, as shown in the right curves. Another remark is that by increasing the nanoparticles fraction, the amount of heat transported by the fluid increases also, due to the improvement in nanofluid thermal conductivity.

Figure 5 depicts the heat transfer coefficient in the inner and the annular space (left curves), as well as the ratio to the heat transfer coefficient corresponding to the circular duct (right curves). The first observation is that the inner heat transfer coefficient increases with the velocity and with the nanoparticles loading. The use of elliptical tubes increases the inner heat transfer coefficient and reduces the outer one. The heat transfer coefficient ratio is computed based on the one corresponding to the circular inner duct with the base fluid flow.

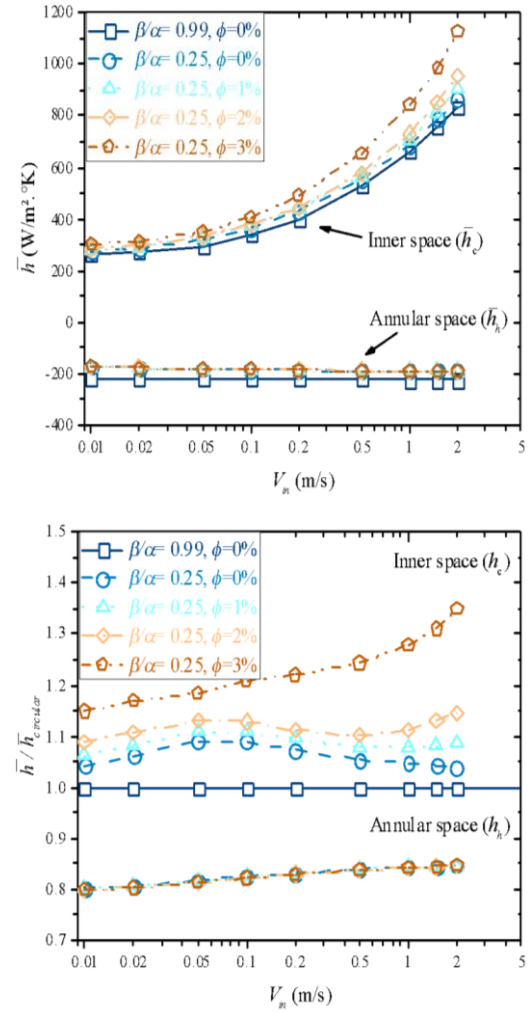


Fig. 5. Effects of velocity, geometry, nanoparticles concentration on the heat transfer coefficient (top) and heat transfer ratio (bottom)

As shown, the use of elliptical duct improves the inner heat transfer coefficient significantly,

and by up to 35% when nanofluid is used; however, the outer heat transfer coefficient decreases by almost 20%. With this data, it is impossible to tell whether there is an improvement in heat exchange or not. Since the two ducts have different areas of the heat transfer surface, we have computed the overall heat transfer coefficient multiplied by the heat exchange area,  $US$ .

The results are depicted in the left-hand curves in Fig. 6, in addition to the ratio (right curves). We observe that in all cases, the elliptical duct exhibits an improvement ranging between 20 and 25%, and of up to 29% when adding nanoparticles.

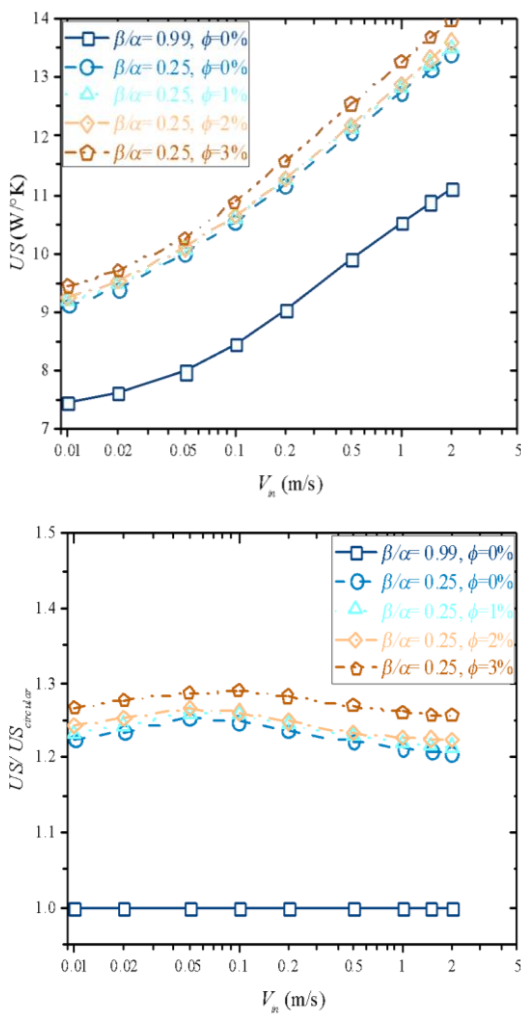


Fig. 6. Variation of the overall heat transfer (top) and its ratio (bottom) in case of elliptical end circular duct

More effective comparisons of the heat exchanger performance can be done by computing the number of transfer unit,  $NTU$  (Fig. 7), and the effectiveness,  $\epsilon$  (Fig. 8).

As shown in Fig. 7, the  $NTU$  starts with a high value and decreases as the velocity increase till it reaches a certain minimum around  $V_{in} = 0.1\text{m/s}$ , then it starts increasing. The same behavior is

observed for the effectiveness in Fig 8. This can be attributed to the change in  $C_{min}$  value as the velocity changes.

At first the cold fluid (the one flowing within the inner pipe), which has a lower heat capacity compared to the hot fluid, is the one controlling the heat transfer. As the velocity increases the cold fluid heat capacity increases till a certain point,  $V_{in} \approx 0.08\text{m/s}$ , where it becomes equal to  $C_h$ , in this phase,  $NTU$  and  $\epsilon$  decrease with the increase of  $V_{in}$ . After this point the fluid controlling the heat transfer is the hot fluid, and the  $NTU$  and  $\epsilon$  start to increase with the velocity.

The second observation is that the use of elliptical duct enhances significantly both the effectiveness and the  $NTU$ . This can be attributed to the increase in the heat exchange area. The elliptical duct's larger surface area compared to a circular duct with the same cross-sectional area promotes enhanced convective heat transfer, leading to improvements in  $NTU$  by 20 to 25% and effectiveness by 2 to 17%. The addition of nanoparticles to the base fluid generates additional improvements, of up to 30% in  $NTU$  and 20% in  $\epsilon$ .

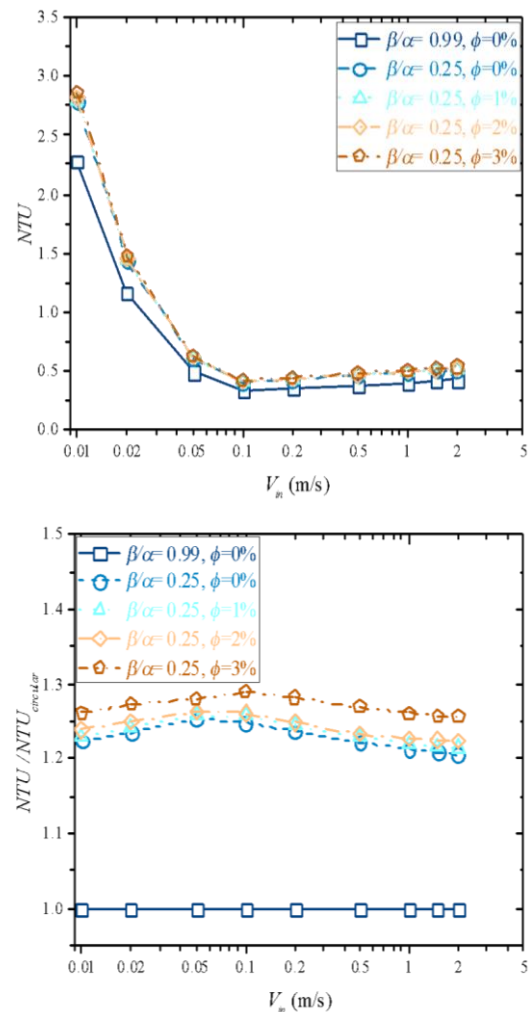
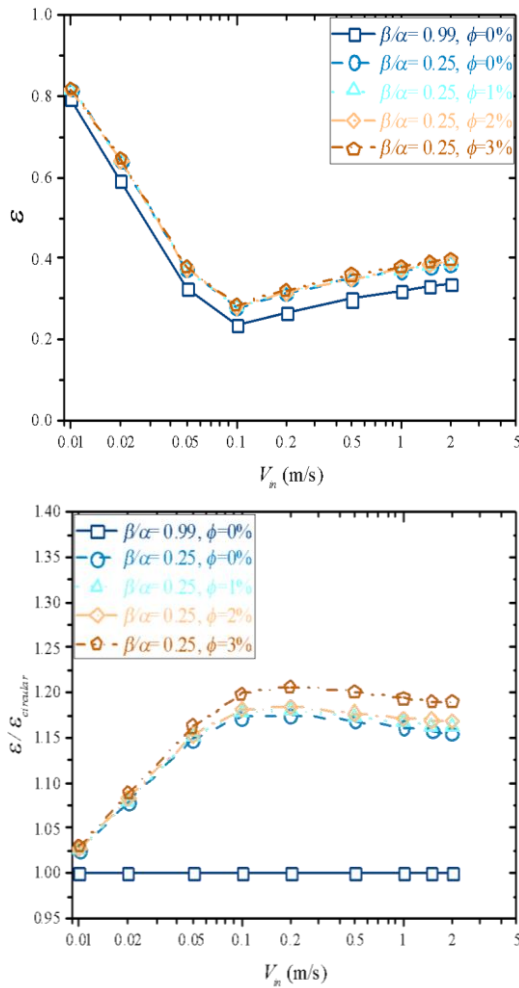


Fig. 7. Variation of  $NTU$  with velocity and enhancement



**Fig. 8.** Effectiveness of the heat exchanger and enhancement using elliptical duct and nanofluids

Since the elliptical duct has a larger exchange surface, technically, it will generate more pressure losses, thus it will require more pumping power. The pressure losses within the inner duct and the required pumping power are computed and depicted in Fig. 9.

From the left-hand curves, we observe that the use of elliptical duct generates more pressure losses, and it increases with the nanoparticles loading for low velocity inlet.

From MWCNT-water experimental data listed in Table 2, this nanofluid exhibits shear-thinning behavior with the addition of nanoparticles. As the MWCNT weight fraction increases, the consistency factor increases whereas the behavior index decreases. For low inlet velocity, the shear rate within the fluid is relatively low, hence, the apparent viscosity is at its highest value, which generates greater pressure losses compared to the Newtonian base-fluid. As the velocity increases, the shear rate increases also; due to the shear-thinning property, the apparent viscosity decreases, thus, it explains why at high velocity the pressure losses for the nanofluid with  $\phi = 3\%$  are lower compared to the base-fluid flow in the circular duct.

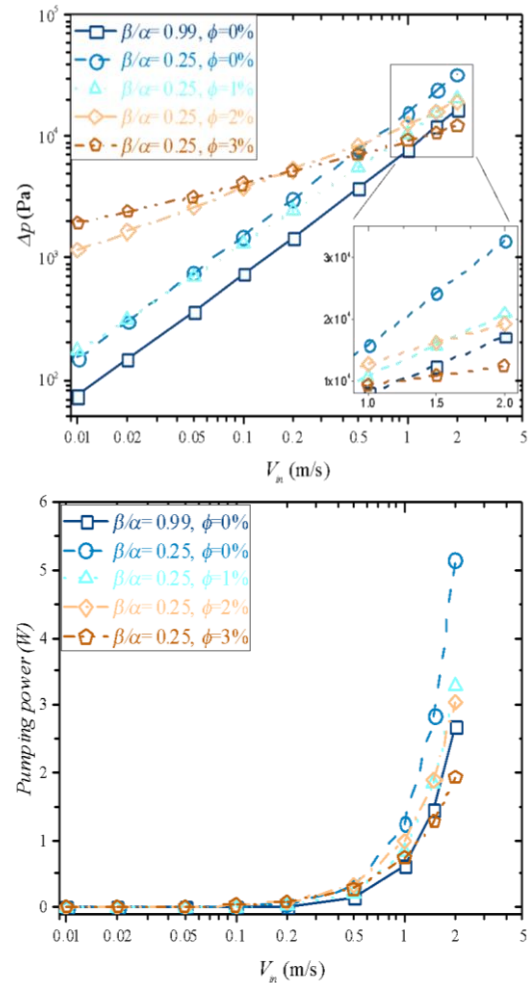


**Fig. 9.** Pressure losses (top) and pumping power (bottom) in the inner duct

The right-hand curves in Fig. 9 depict the pumping power needed by the fluid to flow within the inner duct. For low velocity, despite the pressure losses, the needed power supply is relatively small for all fluids and ducts from the practical view. However, it increases exponentially with the velocity, and it is higher in case of base-fluid flow in elliptical duct. Due to the shear-thinning property of MWCNT-water nanofluid, the amount of required pumping power is reduced and in some cases is lesser than the case of base-fluid flow in circular duct.

## 6. Conclusions

In this chapter, we have conducted a numerical investigation on the effectiveness of the use of elliptical duct and nanofluids in DPHE for the case of co-current flow. The numerical solution was obtained through the use of the finite volume method with consideration of the non-Newtonian fluid flow. The comparisons with the performances of the circular pipe heat exchanger showed that elliptical duct can perform better in terms of the amount of the heat transferred, the outlet temperature, and the

overall heat transfer coefficient. It has been shown that replacing the inner circular pipe with an elliptical pipe improves the number of transfer units up to 25% and the effectiveness up to 17%. Adding nanoparticles to the base fluid improves the amount of the transferred heat and improves the NTU by up to 30% and  $\varepsilon$  by up to 20%.

One inconvenience that has been reported is that elliptical ducts generate more pressure losses; however, the use of non-Newtonian nanofluids reduces this losses and can be more beneficial compared to the base-fluid flow in a circular duct. This is mainly due to the shear-thinning effect caused by the addition of nanoparticles.

The combination of elliptical ducts and non-Newtonian nanofluids offers significant potential for practical applications in industries such as chemical processing, HVAC systems, and renewable energy systems, where enhanced heat transfer efficiency and reduced energy consumption are critical. This approach provides a passive, cost-effective solution for optimizing heat exchanger performance, contributing to energy conservation and sustainable design.

## Nomenclature

$a, b$	Ellipsis major and minor semi-axes' length (m)
$C$	Heat capacity (W/s.K)
$C_p$	Specific heat (J/kg.K)
$D_h$	Hydraulic diameter (m)
$D_{ext}$	External pipe diameter (m)
$h$	Heat transfer coefficient (W/m <sup>2</sup> .K)
$K$	Consistency factor of the power law model (Pa.s $\eta$ )
$L$	Duct length (m)
$\dot{m}$	Masse flow rate (kg/s)
$M$	Mesh configuration
$Nu$	Nusselt number
$NTU$	Number of thermal Unite
$p$	Pressure (Pa)
$Q$	Heat exchanged (W)
$S$	Heat exchange surface (m <sup>2</sup> )
$T$	Temperature (K)
$T_0$	Inlet and wall temperature (K)

$v$	Volume (m <sup>3</sup> )
$U$	Overall heat transfer coefficient (W/m <sup>2</sup> .K)
$V$	Velocity field (m/s)
$x, y, z$	Space coordinates (m)

### Greek symbols

$\dot{\gamma}$	Shear rate
$\varepsilon$	Effectiveness
$\Gamma$	Wall surface (m <sup>2</sup> )
$\eta$	Flow behavior index of the power law model
$\kappa$	Thermal conductivity (W/m.K)
$\Lambda$	Cross-section area (m <sup>2</sup> )
$\mu$	Dynamic viscosity (Pa.s)
$\xi$	Normal vector
$\rho$	Density (kg/m <sup>3</sup> )
$\varphi$	Nanoparticles weight fraction (%)

### Subscripts

$an$	Annular space
$av$	Average
$b$	Bulk
$c$	Cold fluid
$h$	Hot fluid
$i$	Inlet
$in$	Inner space
$min$	Minimum
$o$	Outlet
$w$	Wall

### Superscripts

$-$	Integral average
-----	------------------

## Funding Statement

This research did not receive any specific grant from funding agencies in the public, commercial, or not-for-profit sectors.

## Conflicts of Interest

The author declares that there is no conflict of interest regarding the publication of this article.

## Authors Contribution Statement

*Dounya Behnous*: Conceptualization; Data Curation; Formal Analysis; Investigation; Methodology; Software; Supervision; Roles/Writing – Original Draft; Writing – Review & Editing.

*Haroun Ragueb*: Conceptualization; Investigation; Methodology; Software; Supervision; Validation; Visualization; Roles/Writing – Original Draft; Writing – Review & Editing

*Belkacem Manser*: Visualization; Roles/Writing – Original Draft; Writing – Review & Editing, etc.

*Antar Tahiri*: Investigation; Methodology; Supervision; Validation; Visualization; Roles/Writing – Original Draft; Writing – Review & Editing, etc.

*Kacem Mansouri*: Project administration; Resources; Supervision; Validation; Roles/Writing – Original Draft; Writing – Review & Editing, etc.

## References

- [1] Wijayanta, A.T., Yaningsih, I., Aziz, M., Miyazaki, T. and Koyama, S., 2018. Double-sided delta-wing tape inserts to enhance convective heat transfer and fluid flow characteristics of a double-pipe heat exchanger. *Applied Thermal Engineering*, 145, p. 27-37. <https://doi.org/10.1016/j.applthermaleng.2018.09.009>
- [2] Dandoutiya, B.K. and Kumar, A., 2021. CFD analysis for the performance improvement of a double pipe heat exchanger with twisted tape having triangular cut. *Energy Sources, Part A: Recovery, Utilization, and Environmental Effects*, p. 1-19. <https://doi.org/10.1080/15567036.2021.1946215>
- [3] Gabir, M.M. and Alkhafaji, D., 2021. Comprehensive review on double pipe heat exchanger techniques. *Journal of Physics: Conference Series*, 1973(1), p. 012013. <https://doi.org/10.1088/1742-6596/1973/1/012013>
- [4] Huu-Quan, D., Rostami, A.M., Rad, M.S., Izadi, M., Hajjar, A. and Xiong, Q., 2021. 3D numerical investigation of turbulent forced convection in a double-pipe heat exchanger with flat inner pipe. *Applied Thermal Engineering*, 182, p.116106. <https://doi.org/10.1016/j.applthermaleng.2020.116106>
- [5] Zhang, L., Xiong, W., Zheng, J., Liang, Z. and Xie, S., 2021. Numerical analysis of heat transfer enhancement and flow characteristics inside cross-combined ellipsoidal dimple tubes. *Case Studies in Thermal Engineering*, 25, p.100937. <https://doi.org/10.1016/j.csite.2021.100937>
- [6] Córcoles, J.I., Moya-Rico, J.D., Molina, A.E. and Almendros-Ibáñez, J.A., 2020. Numerical and experimental study of the heat transfer process in a double pipe heat exchanger with inner corrugated tubes. *International Journal of Thermal Sciences*, 158, p.106526. <https://doi.org/10.1016/j.ijthermalsci.2020.106526>
- [7] Luo, C., Song, K. and Tagawa, T., 2021. Heat transfer enhancement of a double pipe heat exchanger by Co-Twisting oval pipes with unequal twist pitches. *Case Studies in Thermal Engineering*, 28, p. 101411. <https://doi.org/10.1016/j.csite.2021.101411>
- [8] Nakhchi, M.E., Hatami, M. and Rahmati, M., 2021. Experimental investigation of performance improvement of double-pipe heat exchangers with novel perforated elliptic turbulators. *International Journal of Thermal Sciences*, 168, p. 107057. <https://doi.org/10.1016/j.ijthermalsci.2021.107057>
- [9] Hashemi Karouei, S.H. and Mousavi Ajarostaghi, S.S., 2021. Influence of a curved conical turbulator on heat transfer augmentation in a helical double-pipe heat exchanger. *Heat Transfer*, 50(2), p. 1872-1894. <https://doi.org/10.1002/htj.21960>
- [10] Noorbakhsh, M., Zaboli, M. and Mousavi Ajarostaghi, S.S., 2020. Numerical evaluation of the effect of using twisted tapes as turbulator with various geometries in both sides of a double-pipe heat exchanger. *Journal of Thermal Analysis and Calorimetry*, 140(3), p. 1341-1353. <https://doi.org/10.1007/s10973-019-08509-w>
- [11] Nakhchi, M.E., Hatami, M. and Rahmati, M., 2021. Effects of CuO nano powder on performance improvement and entropy production of double-pipe heat exchanger with innovative perforated turbulators. *Advanced Powder Technology*, 32(8), p. 3063-3074. <https://doi.org/10.1016/j.apt.2021.06.020>

- [12] Eastman, J.A., Choi, S.U.S., Li, S., Yu, W. and Thompson, L.J., 2001. Anomalous increased effective thermal conductivities of ethylene glycol-based nanofluids containing copper nanoparticles. *Applied physics letters*, 78(6), pp.718-720. <https://doi.org/10.1063/1.1341218>
- [13] Berrehal, H., Karami, R., Dinarvand, S., Pop, I. and Chamkha, A., 2024. Entropy generation analysis for convective flow of aqua Ag-CuO hybrid nanofluid adjacent to a warmed down-pointing rotating vertical cone. *International Journal of Numerical Methods for Heat & Fluid Flow*, 34(2), pp. 878-900. <https://doi.org/10.1108/HFF-05-2023-0236>
- [14] Behrouz, M., Dinarvand, S., Yazdi, M.E., Tamim, H., Pop, I. and Chamkha, A.J., 2023. Mass-based hybridity model for thermomicro-polar binary nanofluid flow: first derivation of angular momentum equation. *Chinese Journal of Physics*, 83, pp.165-184. <https://doi.org/10.1016/j.cjph.2023.03.006>
- [15] Awan, A.U., Majeed, S., Ali, B. and Ali, L., 2022. Significance of nanoparticles aggregation and Coriolis force on the dynamics of Prandtl nanofluid: The case of rotating flow. *Chinese Journal of Physics*, 79, pp.264-274. <https://doi.org/10.1016/j.cjph.2022.07.008>
- [16] Ali, B., Ahammad, N.A., Awan, A.U., Oke, A.S., Tag-Eldin, E.M., Shah, F.A. and Majeed, S., 2022. The dynamics of water-based nanofluid subject to the nanoparticle's radius with a significant magnetic field: The case of rotating micropolar fluid. *Sustainability*, 14(17), p. 10474. <https://doi.org/10.3390/su141710474>
- [17] Noorbakhsh, M., Ajarostaghi, S.S.M., Zaboli, M. and Kiani, B., 2022. Thermal analysis of nanofluids flow in a double pipe heat exchanger with twisted tapes insert in both sides. *Journal of Thermal Analysis and Calorimetry*, 147(5), p. 3965-3976. <https://doi.org/10.1007/s10973-021-10738-x>
- [18] Bahmani, M.H., Akbari, O.A., Zarringhalam, M., Ahmadi Sheikh Shabani, G. and Goodarzi, M., 2020. Forced convection in a double tube heat exchanger using nanofluids with constant and variable thermophysical properties. *International Journal of Numerical Methods for Heat & Fluid Flow*, 30(6), pp. 3247-3265. <https://doi.org/10.1108/HFF-01-2019-0017>
- [19] Arabpour, A., Karimipour, A. and Toghraie, D., 2018. The study of heat transfer and laminar flow of kerosene/multi-walled carbon nanotubes (MWCNTs) nanofluid in the microchannel heat sink with slip boundary condition. *Journal of Thermal Analysis and Calorimetry*, 131(2), p. 1553-1566. <https://doi.org/10.1007/s10973-017-6649-x>
- [20] Zakhast, M., Toghraie, D. and Karimipour, A., 2017. Developing a new correlation to estimate the thermal conductivity of MWCNT-CuO/water hybrid nanofluid via an experimental investigation. *Journal of Thermal Analysis and Calorimetry*, 129(2), p. 859-867. <https://doi.org/10.1007/s10973-017-6213-8>
- [21] Ragueb, H. and Mansouri, K., 2019. Numerical investigation of laminar forced convection for a non-Newtonian nanofluids flowing inside an elliptical duct under convective boundary condition. *International Journal of Numerical Methods for Heat & Fluid Flow*, 29(1), p. 334-364. <https://doi.org/10.1108/HFF-02-2018-0055>
- [22] Akbar, N.S., Zamir, T., Noor, T., Muhammad, T. and Ali, M.R., 2024. Heat transfer enhancement using ternary hybrid nanofluid for cross-viscosity model with intelligent Levenberg-Marquardt neural networks approach incorporating entropy generation. *Case Studies in Thermal Engineering*, 63, p.105290. <https://doi.org/10.1016/j.csite.2024.105290>
- [23] Akbar, N.S., Akram, J., Hussain, M.F., Maraj, E.N. and Muhammad, T., 2024. Thermal storage study and enhancement of heat transfer through hybrid Jeffrey nanofluid flow in ducts under peristaltic motion with entropy generation. *Thermal Science and Engineering Progress*, 49, p. 102463. <https://doi.org/10.1016/j.tsep.2024.102463>
- [24] Moradi, A., Toghraie, D., Isfahani, A.H.M. and Hosseinian, A., 2019. An experimental study on MWCNT-water nanofluids flow and heat transfer in double-pipe heat exchanger using porous media. *Journal of Thermal Analysis and Calorimetry*, 137(5), pp. 1797-1807. <https://doi.org/10.1007/s10973-019-08076-0>
- [25] Hashemi Karouei, S.H., Ajarostaghi, S.S.M., Gorji-Bandpy, M. and Hosseini Fard, S.R., 2021. Laminar heat transfer and fluid flow of

- two various hybrid nanofluids in a helical double-pipe heat exchanger equipped with an innovative curved conical turbulator: SH Hashemi Karouei et al. *Journal of Thermal Analysis and Calorimetry*, 143(2), pp. 1455-1466. <https://doi.org/10.1007/s10973-020-09425-0>
- [26] Fathian, F., Mirjalily, S.A.A., Salimpour, M.R. and Oloomi, S.A.A., 2020. Experimental investigation of convective heat transfer of single and multi-walled carbon nanotubes/water flow inside helical annuli. *Journal of Enhanced Heat Transfer*, 27(3), p. 195-206. <https://doi.org/10.1615/JEnhHeatTransf.2020032605>
- [27] Zainith, P. and Mishra, N.K., 2021. A Comparative Study on Thermal-Hydraulic Performance of Different Non-Newtonian Nanofluids Through an Elliptical Annulus. *Journal of Thermal Science and Engineering Applications*, 13(5) p. 051027. <https://doi.org/10.1115/1.4050235>
- [28] Zainith, P. and Mishra, N.K., 2021. Experimental Investigations on Stability and Viscosity of Carboxymethyl Cellulose (CMC)-Based Non-Newtonian Nanofluids with Different Nanoparticles with the Combination of Distilled Water. *International Journal of Thermophysics*, 42(10), p. 137. <https://doi.org/10.1007/s10765-021-02890-1>
- [29] Zainith, P. and Mishra, N.K., 2021. Experimental investigations on heat transfer enhancement for horizontal helical coil heat exchanger with different curvature ratios using carboxymethyl cellulose-based non-Newtonian nanofluids. *Heat Transfer Research*, 52(16), p. 49-67. <https://doi.org/10.1615/HeatTransRes.2021038864>
- [30] Zainith, P. and Mishra, N.K., 2022. Evaluation of Thermal Performance of Conically Shaped Micro Helical Tubes Using Non-Newtonian Nanofluids—A Numerical Study. *Journal of Thermal Science and Engineering Applications*, 14(8), p. 081019. <https://doi.org/10.1115/1.4054643>
- [31] Namburu, P.K., Kulkarni, D.P., Misra, D. and Das, D.K., 2007. Viscosity of copper oxide nanoparticles dispersed in ethylene glycol and water mixture. *Experimental Thermal and Fluid Science*, 32(2), pp. 397-402. <https://doi.org/10.1016/j.expthermflusci.2007.05.001>
- [32] Teipel, U. and Förter-Barth, U., 2001. Rheology of nano-scale aluminum suspensions. *Propellants, Explosives, Pyrotechnics*, 26(6), p. 268-272. [https://doi.org/10.1002/1521-4087\(200112\)26:6<268::aid-prep268>3.0.co;2-l](https://doi.org/10.1002/1521-4087(200112)26:6<268::aid-prep268>3.0.co;2-l)
- [33] Chen, H., Witharana, S., Jin, Y., Kim, C. and Ding, Y., 2009. Predicting thermal conductivity of liquid suspensions of nanoparticles (nanofluids) based on rheology. *Particuology*, 7(2), pp. 151-157. <https://doi.org/10.1016/j.partic.2009.01.005>
- [34] Chandrasekar, M., Suresh, S. and Chandra Bose, A., 2010. Experimental investigations and theoretical determination of thermal conductivity and viscosity of Al<sub>2</sub>O<sub>3</sub>/water nanofluid. *Experimental Thermal and Fluid Science*, 34(2), p. 210-216. <https://doi.org/10.1016/j.expthermflusci.2009.10.022>
- [35] Chen, H., Yang, W., He, Y., Ding, Y., Zhang, L., Tan, C., Lapkin, A.A. and Bavykin, D.V., 2008. Heat transfer and flow behaviour of aqueous suspensions of titanate nanotubes (nanofluids). *Powder technology*, 183(1), pp. 63-72. <https://doi.org/10.1016/j.powtec.2007.11.014>
- [36] Phuoc, T.X. and Massoudi, M., 2009. Experimental observations of the effects of shear rates and particle concentration on the viscosity of Fe<sub>2</sub>O<sub>3</sub>-deionized water nanofluids. *International Journal of Thermal Sciences*, 48(7), p. 1294-1301. <https://doi.org/10.1016/j.ijthermalsci.2008.11.015>
- [37] Chen, H., Ding, Y., Lapkin, A. and Fan, X., 2009. Rheological behaviour of ethylene glycol-titanate nanotube nanofluids. *Journal of nanoparticle research*, 11(6), pp. 1513-1520. <https://doi.org/10.1007/s11051-009-9599-9>
- [38] Hojjat, M., Etemad, S.G., Bagheri, R. and Thibault, J., 2011. Rheological characteristics of non-Newtonian nanofluids: experimental investigation. *International Communications in Heat and Mass Transfer*, 38(2), pp. 144-148. <https://doi.org/10.1016/j.icheatmasstransfer.2010.11.019>
- [39] Garg, P., Alvarado, J.L., Marsh, C., Carlson, T.A., Kessler, D.A. and Annamalai, K., 2009. An experimental study on the effect of ultrasonication on viscosity and heat transfer performance of multi-wall carbon

- nanotube-based aqueous nanofluids. *International Journal of Heat and Mass Transfer*, 52(21-22), pp. 5090-5101. <https://doi.org/10.1016/j.ijheatmasstransfer.2009.04.029>
- [40] Phuoc, T.X., Massoudi, M. and Chen, R.H., 2011. Viscosity and thermal conductivity of nanofluids containing multi-walled carbon nanotubes stabilized by chitosan. *International Journal of Thermal Sciences*, 50(1), pp. 12-18. <https://doi.org/10.1016/j.ijthermalsci.2010.09.008>
- [41] Ding, Y., Alias, H., Wen, D. and Williams, R.A., 2006. Heat transfer of aqueous suspensions of carbon nanotubes (CNT nanofluids). *International Journal of Heat and Mass Transfer*, 49(1-2), pp. 240-250. <https://doi.org/10.1016/j.ijheatmasstransfer.2005.07.009>
- [42] Ko, G.H., Heo, K., Lee, K., Kim, D.S., Kim, C., Sohn, Y. and Choi, M., 2007. An experimental study on the pressure drop of nanofluids containing carbon nanotubes in a horizontal tube. *International journal of heat and mass transfer*, 50(23-24), pp. 4749-4753. <https://doi.org/10.1016/j.ijheatmasstransfer.2007.03.029>
- [43] Mostafizur, R.M., Aziz, A.A., Saidur, R., Bhuiyan, M.H.U. and Mahbulul, I.M., 2014. Effect of temperature and volume fraction on rheology of methanol based nanofluids. *International Journal of Heat and Mass Transfer*, 77, pp. 765-769. <https://doi.org/10.1016/j.ijheatmasstransfer.2014.05.055>
- [44] Aladag, B., Halefadi, S., Doner, N., Maré, T., Duret, S. and Estellé, P., 2012. Experimental investigations of the viscosity of nanofluids at low temperatures. *Applied energy*, 97, pp. 876-880. <https://doi.org/10.1016/j.apenergy.2011.12.101>
- [45] Ding, Y., Chen, H., He, Y., Lapkin, A., Yeganeh, M., Šiller, L. and Butenko, Y.V., 2007. Forced convective heat transfer of nanofluids. *Advanced Powder Technology*, 18(6), pp.813-824. <https://doi.org/10.1163/156855207782515021>
- [46] Mahbulul, I.M., Khaleduzzaman, S.S., Saidur, R. and Amalina, M.A., 2014. Rheological behavior of Al<sub>2</sub>O<sub>3</sub>/R141b nanorefrigerant. *International Journal of heat and Mass transfer*, 73, pp. 118-123. <https://doi.org/10.1016/j.ijheatmasstransfer.2014.01.073>
- [47] Ragueb, H. and Mansouri, K., 2013. A numerical study of viscous dissipation effect on non-Newtonian fluid flow inside elliptical duct. *Energy Conversion and Management*, 68, p. 124-132. <https://doi.org/10.1016/j.enconman.2012.12.031>
- [48] Maia, C.R.M., Aparecido, J.B. and Milanez, L.F., 2006. Heat transfer in laminar flow of non-Newtonian fluids in ducts of elliptical section. *International Journal of Thermal Sciences*, 45(11), pp. 1066-1072. <https://doi.org/10.1016/j.ijthermalsci.2006.02.001>
- [49] Ragueb, H. and Mansouri, K., 2018. An analytical study of the periodic laminar forced convection of non-Newtonian nanofluid flow inside an elliptical duct. *International Journal of Heat and Mass Transfer*, 127, pp. 469-483. <https://doi.org/10.1016/j.ijheatmasstransfer.2018.07.051>
- [50] Ragueb, H. and Mansouri, K., 2023. Exact solution of the Graetz-Brinkman problem extended to non-Newtonian nanofluids flow in elliptical microchannels. *Journal of Engineering Mathematics*, 140(1), p. 10. <https://doi.org/10.1007/s10665-023-10267-6>
- [51] Abdel-Wahed, R.M., Attia, A.E. and Hifni, M.A., 1984. Experiments on laminar flow and heat transfer in an elliptical duct. *International journal of heat and mass transfer*, 27(12), pp. 2397-2413. [https://doi.org/10.1016/0017-9310\(84\)90098-X](https://doi.org/10.1016/0017-9310(84)90098-X)
- [52] Javeri, V., 1976. Analysis of laminar thermal entrance region of elliptical and rectangular channels with Kantorowich method. *Wärme-Und Stoffübertragung*, 9(2), pp. 85-98. <https://doi.org/10.1007/bf01589462>
- [53] Matos, R.S., Laursen, T.A., Vargas, J.V.C. and Bejan, A., 2004. Three-dimensional optimization of staggered finned circular and elliptic tubes in forced convection. *International Journal of Thermal Sciences*, 43(5), pp. 477-487. <https://doi.org/10.1016/j.ijthermalsci.2003.10.003>
- [54] Matos, R.S., Vargas, J.V.C., Laursen, T.A. and Bejan, A., 2004. Optimally staggered finned circular and elliptic tubes in forced convection. *International Journal of Heat and Mass Transfer*, 47(6-7), pp. 1347-1359. <https://doi.org/10.1016/j.ijheatmasstransfer.2003.08.015>

- [55] Li, Z., Davidson, J.H. and Mantell, S.C., 2006. Numerical simulation of flow field and heat transfer of streamlined cylinders in cross flow. *Journal of Heat Transfer*, 128(6), p. 564-570. <https://doi.org/10.1115/1.2188463>
- [56] Ibrahim, T.A. and Gomaa, A., 2009. Thermal performance criteria of elliptic tube bundle in crossflow. *International Journal of Thermal Sciences*, 48(11), pp. 2148-2158. <https://doi.org/10.1016/j.ijthermalsci.2009.03.011>
- [57] Mohanan, A.K., Prasad, B.V. and Vengadesan, S., 2021. Flow and heat transfer characteristics of a cross-flow heat exchanger with elliptical tubes. *Heat Transfer Engineering*, 42(21), pp. 1846-1860. <https://doi.org/10.1080/01457632.2020.1826742>
- [58] Chien, L.H., Chen, D.C., Liu, Y.J., Yan, W.M. and Ghalambaz, M., 2021. Heat and mass transfer of evaporative cooler with elliptic tube heat exchangers-an experimental study. *International Communications in Heat and Mass Transfer*, 127, p. 105502. <https://doi.org/10.1016/j.icheatmasstransfer.2021.105502>
- [59] Patankar, S., 2018. *Numerical heat transfer and fluid flow*. Taylor & Francis, CRC press.
- [60] Chhabra, R.P. and Patel, S.A., 2025. *Non-Newtonian flow and applied rheology: engineering applications*. Elsevier.
- [61] Eymard, R., Gallouët, T. and Herbin, R., 2000. Finite volume methods. *Handbook of numerical analysis*, 7, pp. 713-1018.
- [62] Shah, R.K. and Sekulic, D.P., 2003. *Fundamentals of heat exchanger design*. John Wiley & Sons.
- [63] Tahiri, A., Ragueb, H., Moussaoui, M., Mansouri, K., Guerraiche, D. and Guerraiche, K., 2024. Heat transfer and entropy generation in viscous-joule heating MHD microchannels flow under asymmetric heating. *International Journal of Numerical Methods for Heat & Fluid Flow*, 34(10), pp. 3953-3978. <https://doi.org/10.1108/HFF-05-2024-0380>
- [64] Ragueb, H., Tahiri, A., Behnous, D., Manser, B., Rachedi, K. and Mansouri, K., 2023. Irreversibilities and heat transfer in magnetohydrodynamic microchannel flow under differential heating. *International Communications in Heat and Mass Transfer*, 149, p. 107155. <https://doi.org/10.1016/j.icheatmasstransfer.2023.107155>
- [65] Rachedi, K., Ragueb, H., Behnous, D., Tahiri, A., Manser, B. and Ait Chikh, M.A., 2026. Analysis of natural convection heat transfer in a rectangular cavity with discrete heat flux: Implications for building thermal management using artificial neural networks. *Numerical Heat Transfer, Part B: Fundamentals*, 87(1), p. 2389215. <https://doi.org/10.1080/10407790.2024.2389215>
- [66] Chhabra, R.P., 2010. Non-Newtonian fluids: an introduction. In *Rheology of complex fluids* (pp. 3-34). New York, NY: Springer New York.
- [67] Bennett, T.D., 2019. Correlations for the Graetz problem in convection-Part 1: For round pipes and parallel plates. *International Journal of Heat and Mass Transfer*, 136, pp. 832-841. <https://doi.org/10.1016/j.ijheatmasstransfer.2019.03.006>